Published in final edited form as:
Biomaterials. 2011 August ; 32(22): 5056–5064. doi:10.1016/j.biomaterials.2011.03.054.

The role of substratum compliance of hydrogels on vascular endothelial cell behavior

Joshua A. Wood[a], **Nihar M. Shah**[a], **Clayton T. McKee**[a], **Marissa L. Hughbanks**[a], **Sara J. Liliensiek**[b], **Paul Russell**[a], and **Christopher J. Murphy**[a,c,*]

[a]Department of Surgical and Radiological Sciences, School of Veterinary Medicine, 1 Shields Avenue, University of California, Davis, CA 95616, USA

[b]Department of Chemical and Biological Engineering, School of Engineering, University of Wisconsine–Madison, USA

[c]Department of Ophthalmology and Vision Sciences, School of Medicine, University of California, Davis, CA 95616, USA

Abstract

Cardiovascular disease (CVD) remains a leading cause of death both within the United States (US) as well as globally. In 2006 alone, over one-third of all deaths in the US were attributable to CVD. The high prevalence, mortality, morbidity, and socioeconomic impact of CVD has motivated a significant research effort; however, there remain significant knowledge gaps regarding disease onset and progression as well as pressing needs for improved therapeutic approaches. One critical area of research that has received limited attention is the role of biophysical cues on the modulation of endothelial cell behaviors; specifically, the impact of local compliance, or the stiffness, of the surrounding vascular endothelial extracellular matrix. In this study, the impact of substratum compliance on the modulation of cell behaviors of several human primary endothelial cell types, representing different anatomic sites and differentiation states *in vivo*, were investigated. Substrates used within our studies span the range of compliance that has been reported for the vascular endothelial basement membrane. Differences in substratum compliance had a profound impact on cell attachment, spreading, elongation, proliferation, and migration. In addition, each cell population responded differentially to changes in substratum compliance, documenting endothelial heterogeneity in the response to biophysical cues. These results demonstrate the importance of incorporating substratum compliance in the design of *in vitro* experiments as well as future prosthetic design. Alterations in vascular substratum compliance directly influence endothelial cell behavior and may participate in the onset and/or progression of CVDs.

Keywords

Endothelial cell; Compliance; Biomimetic material; Bioprosthesis; Cell viability; Vascular grafts

*Corresponding author. Department of Surgical and Radiological Science, School of Veterinary Medicine, 1 Shields Avenue, University of California, Davis, CA 95616. Tel.: +1 530 754 0216. murphyc@corl.vetmed.wisc.edu, cjmurphy@ucdavis.edu (C.J. Murphy).

1. Introduction

Cardiovascular disease (CVD) is defined as a group of vascular disorders that involve the heart as well as the vasculature. CVD remains the leading cause of death in developed nations and accounts for over one-third of all deaths within the United States each year [1]. In addition, the estimated financial cost of CVD for 2010, within the US, is expected to exceed $500 billion [1]. Both the humanitarian and financial costs associated with treatment of CVD have motivated a significant research effort aimed at increasing understanding of disease onset and progression as well as improving treatment and patient outcome. The currently available therapies for CVD include systemic medication and/or surgical intervention depending on the severity of the case and nature of the disease process. Despite these advances, there remains a critical need for improvements in existing therapeutic regimens, which includes the development of improved vascular prosthetics [2,3].

The most common surgical option for treatment of vascular disorders involves vessel transplantation from the host or donor tissue [4]. However, when host or donor vascular tissue is not available, synthetic grafts are utilized as an alternative. Despite improvements in current synthetic graft design, significant rates of graft failure occur due to the onset of thrombosis associated with regions with inadequate coverage of endothelium [3]. Current designs of vascular grafts have focused on mimicking the known bulk resistance to deformation of native vessel tissue from blood flow through the vessel. However, these devices have not generally integrated localized biophysical cues in their design parameters. Biophysical attributes of the substratum directly influence endothelial cell behaviors. One must also be aware of the experimental method by which a resistance to applied stress is measured [5] i.e. it would not be appropriate to use tensile measures of bulk vessel compliance to investigates how endothelial cells respond to the local microscopic and nanoscopic compliance of vessel tissue.

The native basement membrane (BM), through which vascular endothelial cells attach to the underlying stroma, provides both chemical and biophysical cues to the overlying endothelial cells [6]. Biophysical attributes of the BM have been shown to modulate essential endothelial cell behaviors [7–10]. For example, the stiffness of the BM and subjacent matrix has been reported to modulate a variety of endothelial cell behaviors and functions that are important for cell survival, replication, migration, and general tissue homeostasis [3]. While a complete study of the local compliance of the various vascular BMs has yet to be performed, several authors have published values from various species and vessel types. While variations in reported values exist, the Young's modulus for healthy vascular BM from currently published work provides a range of approximately 2.5–70 kPa [3,11–17]. These previous studies demonstrate the need for further investigation into the biophysical properties of the basement membrane and the impact on endothelial cell behavior.

Recent reports have also suggested that dysregulation of the endothelial layer can result in modification of the extracellular matrix (ECM) and influence disease states [3,18]. For example, in atherogenesis, both softening and stiffening of the basement membrane have been reported [3,8,19]. Several other diseases including Alzheimer's, cerebral vascular disease, and certain forms of diabetes lead to alterations in the thickness and pliability of the vascular basement membrane as well [20–23]. These reports demonstrate the dynamic interaction between the ECM and the overlying endothelial cells and the potential impact on a menu of fundamental cell behaviors including adhesion, alignment, orientation, proliferation, and migration [24,25].

It has been well established that vascular endothelial cell populations throughout the body are not homogenous [26]. The response of cells can vary depending on their site of origin

such as large or small vessels, exposure to forces including flow, and their function within the vascular tissue [3,8,27]. Differences in endothelial behaviors are important for both the elucidation of mechanisms involved in the onset and progression of disease as well as in developing therapeutic approaches for re-establishment of a functional endothelial layer post vascular transplant.

To address heterogeneity of endothelial cells in our studies examining biophysical cues, we employed primary human endothelial cells from umbilical vein (HUVEC), aorta (HAEC), saphenous vein (HSaVEC), and dermal microvasculature (HmVEC). These primary cells served as representative populations from early progenitor cells, major arteries and veins, and microvasculature, respectively. The effect of substrate stiffness on each unique population of endothelial cells is important for the development of artificial conduits that posses optimal physical properties appropriate for each vessel type. Substratum stiffness is known to change in certain disease states and a better understanding of the response of endothelial cells to alterations in substrate stiffness could shed new light on the development of CVD. The study reported herein was undertaken to detail the modulation of fundamental endothelial cell behaviors by the local modulus of the underlying substrata.

2. Materials and methods

2.1. Cell culture

Umbilical vein (HUVEC), aorta (HAEC), saphenous vein (HSaVEC) (Promocell, Heidelberg, Germany), and dermal microvasculature (HmVEC) endothelial cells (Lonza, Walkerville, MD) were investigated. Cells were used between passages 2 and 7 for all experiments. Endothelial basal media supplemented with the EGM-2 BulletKit containing: GA-1000, hEGF, fetal bovine serum, heparin, ascorbic acid, R3-IGF, VEGF, hFGF-B, and hydrocortisone (Lonza, Walkerville, MD) were used to culture the HUVECs, HAECs, and HSaVECs. HmVEC's were cultured in, endothelial basal medium supplemented with the EGM-2 MV BulletKit containing: ascorbic acid, R3-IGF1, hFGF-B, VEGF, FBS, GA-1000, hydrocortisone, and hEGF. Cell cultures were incubated at 37 °C and 5% CO_2.

2.2. Hydrogel fabrication

To investigate the effects of BM stiffness on endothelial cell behaviors, a series of polyacrylamide gels that range in modulus from 25 to 75 kPa were fabricated [28]. Hydrogels of three different compliance values (25, 50, and 75 kPa) were synthesized by combining pre-mixed solutions of acrylamide (Am) and N,N′-methyl-enebisacrylamide (BIS) (Am:BIS 29:1, 40%, Fisher, Waltham, MA), with 400 μl of (3-acrylamidepropyl)trimethylammonium chloride (API, 75% w/w, Sigma, Carlsbad, CA) by gently swirling. The range of substrate compliancewas created by varying the cross-linker density [6,29]. Immediately, 200 μl of 10% w/v solution of ammonium persulfate (initiator, APS, Fisher, Waltham, MA) was added to the above solutions and mixed until the solution became completely transparent followed by addition of 30 μl of the catalyst (tetramethylethylenediamine, TEMED, 99%, Sigma, Carlsbad, CA). The solutions were gently swirled and quickly poured into empty gel casting cassettes (1 mm thickness, Bio-Rad, Hercules, CA) and allowed to gel for 60 min. The top centimeter of gel closest to the air interface was discarded due to variation in the resultant compliance of this region compared to the rest of the gel.

To remove unreacted reagents, the cut gels were rinsed three times in 1× phosphate buffered saline (PBS, HyClone, Fisher Scientific, Waltham, MA). The gels were then sterilized in a hydrated state by exposure to short wavelength (280 nm) UV light for 30 min. Following an additional PBS rinse, the substrates were stored in a 5% CO_2 incubator at 37 °C for at least

24 h followed by one additional 1× PBS rinse and 24 h incubation to attain full hydration. The gels were then placed in the appropriate serum containing medium for 24 h to attain full equilibrium and subsequently coated with fibronectin and collagen (FNC, AthenaES, Baltimore, MD) prior to seeding cells.

2.3. Measurement of hydrogel compliance

The mechanical properties of our synthesized hydrogels were quantified following the hydration step by measuring the Young's elastic modulus using an atomic force microscope (AFM) (MFP-3D-BIO, Asylum Research, Santa Barbara, CA) [30]. The resistance to deformation of the hydrogels was quantified by monitoring the force required to indent the surfaces, using silicon nitride cantilevers (PNP-TR-50, k = 60 pN/nm, NanoAndMore, Lady's Island, SC) that have a square pyramid tip. Young's modulus was determined by fitting these force vs. indentation curves using Equation (1) [31]:

$$E=\frac{\pi F(1-\upsilon^2)}{2\tan(\alpha)\delta^2} \quad (1)$$

Where E is Young's Modulus, F is the force, δ is the depth of indentation, α is half angle opening of the cantilever tip, and ν is Poisson's ratio of the hydrogel, which we assumed to be 0.5 [32]. For each gel, five separate locations were probed, with a minimum of five force vs. indentation curves measured at each location. These forces curves were averaged together to determine the average and standard deviation of Young's modulus from Equation (1). The hydrogels used in this study mimic both healthy (homeomimetic) and disease (pathomimetic) states based on the currently published range of vascular basement membrane compliances of 2.5–70 kPa [3,11–17]. The elastic modulus of the hydrogels used were 28 ± 4 kPa, 52 ± 7 kPa, and 71 ± 5 kPa.

2.4. Microscopy

A Zeiss Axiovert 200 M inverted microscope with a motorized stage, a 10X/0.4NA lens, AxioCam HRm or AxioCam b/w (Carl Zeiss Inc., North America) was used for image acquisition for studies related to cell attachment, cell area proliferation, and migration assays. HUVEC, HSaVEC, and HmVEC cell images were collected using the AxioCam b/w monochromatic camera using a 10X/0.3NA lens with 2 × 2 binning. All HAEC cell images were collected using the AxioCam HRm using a 10X/0.3NA lens with 2 × 2 binning. Phase contrast imaging was used for all image acquisition and the Zeiss migration tracking package was used in the migration analysis.

2.5. Cell adhesion assay

Following preparation of the hydrogels, 30,000 cells were seeded onto each 0.5 inch diameter hydrogel disk and incubated for 24 h. Four phase contrast images were then taken from separate regions. The total number of cells attached to the surface in each image was quantitated using Image J version 1.42q with the cell counter plug-in (NIH, Bethesda, MD). We included a total of 9–12 gels for a given modulus (4 images each) for each experiment. Each experiment was repeated in triplicate for a total of 30–36 gels of a given modulus and endothelial cell type. The averages from each of the three compliant gels and tissue culture plastic (TCP) controls were then analyzed for statistical significance between treatments.

2.6. Analysis of cell area and elongation

Inclusion criteria for the cell area and elongation factor assays required cells to be adherent, with no discernable cleavage furrows, and having no cell–cell contact with other cells. The perimeters of each adherent cell were traced using Image J ver. 1.42q (NIH, Bethesda, MD).

Using the free hand trace function, a total of 150–170 cells for a given modulus and cell type acquired from 9 to 12 gels in each of three replicates (33–36 gels total per modulus) were traced. The measurement plug-in from Image J was then used to measure the total area of each traced cell as well as the ratio of the major axis/minor axis of each cell based on a fitted ellipse model.

2.7. Proliferation assay

In the cell proliferation assay, cells were plated (same density as above) and cultured on our compliant hydrogel substrates for five days. For each endothelial cell strain, images were acquired 1 day and 5 days after plating. The percent increase in cell number and subsequent proliferation was determined by subtracting the cell number present at day 1 from day 5 and dividing the result by the number of cells present on day one [8]. A total of 30–36 gels per modulus for each cell type were used in this assay.

2.8. Migration assay

Triple-pack gel dishes were used as illustrated in Fig. 1. One gel substrate of each compliance value (25, 50 and 75 kPa) was placed inside a 35 mm dish and prepared as previously described. For the migration assays, hydrogel substrates were prepared as previously described and seeded with 5000–50,000 cells depending on gel diameter and modulus to obtain 30–40% confluence 1 h after seeding [8]. Cells were then imaged every 10 min over the course of 12 h in a heated, 5% CO_2 microscope chamber using the position list, and time lapse applications of the Axiovision software package. The tracking analysis module of the Axiovision software was used to track all fully adherent cells not in contact with another cell. A total of 60–258 cells per substrate were tracked from at least three separate experiments.

2.9. Statistics

All data were analyzed using the Sigma Plot 11 software package (Systat Software, Chicago, IL). Analysis of variance (ANOVA) was the primary analysis method using the Tukey post-hoc test or Kruskal–Wallis ANOVA on ranks with Dunn's post-hoc modification depending on the results of the normality test. In addition, two-tailed Students' *t*-tests and Mann–Whitney rank sum tests were employed depending on the results of Chi-square normality tests. All levels of significance were determined when * = $p < 0.05$, ** = $p < 0.01$, or *** = $p < 0.001$.

3. Results

Several key cellular behaviors were differentially modulated by substratum compliance including:

3.1. Cell adhesion

The impact of substrate compliance on endothelial cell attachment varied with the endothelial cell type investigated. HUVEC attachment on the 75 kPa hydrogel surfaces was significantly lower than on any of the other surfaces (Fig. 2A). Compared to 75 kPa substrates, the number of cells/field was increased by 2.6–3.2 fold on 25 kPa, 50 kPa, and TCP (>1 GPa). HmVEC cells exhibited similar results with lowest total cell numbers on the 75 kPa surfaces. In contrast to HUVECs and HmVECs, HAECs (Fig. 2C) attached best to 50 kPa substrates. HSaVEC cell attachment was equivalent on the 25 kPa, 50 kPa and 75 kPa surfaces with greatest attachment being observed on TCP (Fig. 2D).

3.2. Cell morphology and elongation

HUVECs on 75 kPa surfaces were smaller and more round in appearance than HUVECs on either 25 kPa or TCP surfaces. The density of actin stress fibers was greatest on TCP substrates compared to compliant hydrogels (Fig. 3) [29,33]. In general, all cells exhibited the greatest surface area on TCP with the effect of hydrogel compliance on surface area varying with the cell type investigated. HUVECs and HmVECs had the smallest surface area on the 75 kPa hydrogels (Fig. 4A and B). In contrast to these findings, the cell area measurements for arterial cells (HAECs) were smaller on the 25 kPa surfaces compared to the 50 kPa ($p < 0.001$) surfaces but not significantly different than the cells on the 75 kPa surfaces (Fig. 4C). HSaVECs on the 50 kPa surfaces were larger ($p < 0.01$) than cells on the 75 kPa surfaces and similar in size to those cells on the 25 kPa surfaces (Fig. 4D).

Overall, substrate compliance was found to influence cell elongation. Generally, cells exhibited the greatest elongation on the softest (25 kPa) substrates (Fig. 5). HUVECs (Fig. 5A) seeded onto 75 kPa and 50 kPa surfaces were significantly more rounded than those cells seeded onto 25 kPa and TCP surfaces ($p < 0.001$). HmVECs (Fig. 5B) seeded onto 50 kPa surfaces were significantly more rounded than cells seeded onto TCP. HmVEC cells on the 25 kPa and 75 kPa substrates were similar to the cells on the 50 kPa surfaces. HAECs (Fig. 5C) seeded onto 25 kPa surfaces were significantly more elongated than cells seeded onto 50 kPa ($p < 0.001$) and 75 kPa ($p < 0.01$) surfaces. In contrast, HAECs were not significantly elongated on any surfaces. Finally, HSaVECs (Fig. 5D) seeded on to 25 kPa surfaces were significantly more elongated than cells on 50 kPa, 75 kPa, and TCP surfaces ($p < 0.001$). HSaVECs seeded onto 75 kPa surfaces were also significantly more elongated than cells seeded onto TCP surfaces ($p < 0.001$). Overall, the data demonstrate that endothelial cells are more elongated on the softer 25 kPa surfaces compared to 50 kPa, 75 kPa, and TCP.

3.3. Proliferation

Overall, all endothelial cell types proliferated at a slower rate on the hydrogels as compared to control TCP substrates (Fig. 6). At the end of the proliferation assay approximately twice as many cells were present on TCP compared to all hydrogels. Cell line differences were also observed; proliferation of HUVECs was equivalent on all hydrogels whereas HmVECs displayed a marked suppression on the softest (25 kPa) hydrogel substrates and HAECs demonstrated a significant increase on 75 kPa substrates compared to more compliant hydrogels. Overall, these data demonstrate that substrate moduli impact proliferation in a profound manner.

3.4. Migration

Migration was affected by the substrate stiffness as well as the cell type investigated. Overall, after 12 h, cell migration rates were greater on the hydrogels compared to TCP for the HUVECs, HAECs, and HSaVECs (Fig. 7). In contrast, HmVEC migration rates did not vary significantly between the 25 kPa, 50 kPa, 75 kPa, or TCP surfaces (Fig. 7B). In contrast to the HUVECs and HAECs, HSaVECs exhibited faster rates of migration on softer substrates with the fastest rate being observed on the 25 kPa and 50 kPa surfaces (Fig. 7D).

4. Discussion

Vascular endothelial cells (VECs) that form a monolayer lining vascular tissue are not homogenous with regards to behavior or function [3,8,26,27]. Our results document that the heterogeneity in VEC populations is also reflected in their response to the compliance of the substratum. This finding is in line with a recent report from our laboratories documenting variation in VEC response to surface topographic features. The impact of features varied

with: 1.) the cell behavior being considered, 2.) topographic feature scale, 3.) surface order, 4.) and the anatomic origin of the cell being investigated [8]. Not only does the cell response to a given biophysical cue vary depending on anatomic origin, the nanoscale architecture of the vascular basement membrane also varies with anatomic location. We recently reported significant differences ($p < 0.05$) in basement membrane thickness and that pore and fiber diameter correlate with differences in the anatomic location and physical properties of the vessel [7].

The majority of published values for the moduli of vascular basement membranes reside in the range of 2.5–70 kPa [3,11–17]. This is similar to values reported for corneal basement membranes as well as Matrigel, a basement membrane-like complex [34,35]. There are a few publications reporting markedly higher values from 100 + kPa to greater than 1 MPa [14,36]. It is likely that the differences in values for modulus are related to differences in the analytic measurement methods used [5]. The modulus of basement membranes associated with atherosclerotic lesions has been published in rabbits with the moduli of lesions being ≥ 75 kPa compared to a value of 25 kPa for non-affected regions [19]. Our compliant substrates encompassed a range of moduli from normal (25 kPa) to stiffer substrates (75 kPa) approximating those found in vascular disease states. TCP (having a modulus of >1 GPa) was included as a reference substrate as the great majority of *in vitro* experiments continue to be conducted on this material possessing a modulus that far exceeds anything found in biologic tissues.

By studying adhesion, surface area, elongation, proliferation, and migration we have shown the effect of substratum modulus on endothelial cell behaviors and their response to changes in the biophysical properties of the underlying substrate. The stiffness of a substrate has been previously shown to impact endothelial cell adhesion on substrates with moduli that were not biologically relevant [37]. By limiting the compliance of the materials studied to those that are found in native tissues, we have identified specific moduli that optimize cell attachment; a critical factor in the formation of a healthy endothelium on either synthetic matrices or denuded areas of native vessels (Fig. 2). This is a significant advance over previous studies which did not take into account the much softer modulus of the native basement membrane or the heterogeneity of endothelial cell populations [37]. Overall, all endothelial cells from venous locations demonstrated dramatically decreased initial cell attachment on the stiffer 75 kPa surfaces. In contrast, the arterial cell (HAEC) source did not demonstrate a statistically relevant difference despite a higher initial cell density on the 25 kPa and 50 kPa hydrogels. These data suggest that a softer 25 kPa surface provides more ideal conditions toward the formation of a healthy and confluent endothelial layer for venous cell sources.

Characteristics such as cell size and migration are important during the re-population of an extracellular matrix denuded of endothelium as they influence overall cell viability and behavior [38,39]. Specifically, cell size has been correlated with migration at the leading edge of migrating endothelium [40,41]. Our results demonstrate that decreased cell size was observed on the stiffer 75 kPa surfaces compared to the softer 25 kPa or 50 kPa surfaces for each cell type included in our study (Fig. 4). For arterial cell sources, the 50 kPa surfaces contained larger cells than either the 25 kPa or 75 kPa surfaces. In aggregate, these data, in the context of the results observed on initial cell density, demonstrate that the softer 25 kPa surface appears optimal for all venous endothelia tested including HUVECs, HmVECs, and HSaVEC. In contrast, the data suggest that arterial cell types, such as HAECs, are better suited to 50 kPa surfaces.

Endothelial cells with long processes, and thus higher elongation factors, are found in angiogenic regions of vascular tissues and have increased migration rates [8,39].

Additionally, elongated endothelial cells have been shown to have: a lower inflammatory state, decreased ICAM expression, and are less atherogenic. All of these factors are critical to the success of prosthetics and the maintenance of homeostasis in endothelia that have recently re-populated a denuded region of vessel [27,42,43]. Significantly higher elongation factors associated with cells on the 25 kPa surfaces in the HUVEC, HAEC, and HSaVEC cell populations demonstrate their ability to better re-populate areas of denuded endothelium and are in agreement with the other findings that lead to the prediction that the inner wall of vascular prosthetics in intimate association with the VECs should possess moduli in the range of 25–50 kPa for optimal performance (Fig. 5).

The use of biomimetic hydrogels not only informs prosthetic design, but more accurately reflects *in vivo* conditions compared to TCP. Endothelial cells are known to proliferate rapidly *in vitro* but the impact of compliant, biomimetically relevant surfaces on the various types of endothelial cells and their respective proliferation rates has not been measured to date. This information is important for as it demonstrates that the use of biomimetically complaint substrates significantly impacts cell culture results (Fig. 6). This evidence strongly argues for the employment of substrates possessing biologically relevant physical attributes for *in vitro* assays to more accurately reflect *in vivo* conditions.

Endothelial migration results from extension of cell processes on the leading edge of the cell and the cell body moving forward as a result of tractional forces. The increased migration rate that results from using biomimetically relevant compliant substrates further supports incorporation of these important biophysical attributes into the design parameters of vascular prosthetics. With the exception of HmVECs, we found that cell migration rates were increased on 25 kPa and 50 kPa surfaces compared to TCP surfaces (Fig. 7). These results demonstrate that the inclusion of biomimetically relevant physical attributes improves the migration rate of the majority of endothelial cell types studied. These data contribute to the growing body of literature documenting that the results obtained using standard *in vitro* techniques employing TCP may not accurately reflect the *in vivo* condition. Furthermore, a recent report documents that the compliance of the underlying substratum can modulate the response of cells to therapeutic agents [33].

Vascular disease states have been shown to have increased basement membrane stiffness [3,19]. This suggests the possibility that alterations in basement membrane stiffness may participate directly in the initiation and/or progression of CVD. The data obtained in our studies suggest differing optimal substratum moduli for different endothelial populations and also suggest that changes in compliance associated with disease onset and progression may directly participate in CVD.

5. Conclusion

The net results of these experiments show that biomimetically relevant substrates dramatically impact a menu of endothelial cell behaviors. The data suggest that experimental results obtained would profoundly differ when employing substrates with more biomimetic biophysical attributes compared to TCP. The VECs interact with their underlying basement membrane and given the variety of behaviors we have shown to be regulated by inclusion of biologically relevant substratum moduli, inclusion of substratum biophysical cues in cell culture assays would appear imperative. The provision of relevant moduli would likely improve the predictive value of *in vitro* experiments. Substratum stiffness has been shown to change during the development of atherosclerotic lesions and our results suggest that such changes may participate directly in the initiation and/ or progression of CVD.

Acknowledgments

This work was supported by the National Institute of Health through grants from the National Heart, Lung, and Blood Institute (1R01HL079012-01A), the National Eye Institute (1R01EY017367-01A, 1R01EY19475, P30EY12576), and an unrestricted grant from Research to Prevent Blindness. We would also like to thank Oscar Cheung for making many of the gels used in this study and Irene Ly for her help with the cell tracking experiments.

References

1. Lloyd-Jones D, Adams RJ, Brown TM, Carnethon M, Dai S, De Simone G, et al. Heart disease and stroke statistics–2010 update: a report from the American heart association. Circ. 2010; 121(7):e46–e215.
2. L'Heureux N, Dusserre N, Konig G, Victor B, Keire P, Wight TN, et al. Human tissue-engineered blood vessels for adult arterial revascularization. Nat Med. 2006; 12(3):361–365. [PubMed: 16491087]
3. Wood JA, Liliensiek SJ, Russell P, Nealey PF, Murphy CJ. Biophysical cueing and vascular endothelial cell behavior. Materials. 2010; 3(3):1620–1639.
4. Campbell GR, Campbell JH. Development of tissue engineered vascular grafts. Curr Pharm Biotechnol. 2007; 8:43–50. [PubMed: 17311552]
5. McKee CT, Last JA, Russell P, Murphy CJ. Indentation versus tensile measurements of young's modulus for soft biological tissues. Tissue Eng B. in press.
6. Discher DE, Janmey P, Wang YL. Tissue cells feel and respond to the stiffness of their substrate. Science. 2005; 310(5751):1139–1143. [PubMed: 16293750]
7. Liliensiek SJ, Nealey P, Murphy CJ. Characterization of endothelial basement membrane nanotopography in rhesus macaque as a guide for vessel tissue engineering. Tissue Eng A. 2009; 15(9):2643–2651.
8. Liliensiek SJ, Wood JA, Yong J, Auerbach R, Nealey PF, Murphy CJ. Modulation of human vascular endothelial cell behaviors by nanotopographic cues. Biomaterials. 2010; 31:5418–5426. [PubMed: 20400175]
9. Ghajar CM, Chen X, Harris JW, Suresh V, Hughes CCW, Jeon NL, et al. The effect of matrix density on the regulation of 3-D capillary morphogenesis. Biophys J. 2008; 94(5):1930–1941. [PubMed: 17993494]
10. Griffith LG, Swartz MA. Capturing complex 3D tissue physiology in vitro. Nat Rev Mol Cel Biol. 2006; 7:211–223.
11. Ebenstein DM, Pruitt LA. Nanoindentation of soft hydrated materials of application to vascular tissues. J Biomed Mater Res. 2004; 69A:222–232.
12. Engler AJ, Richert L, Wong JY, Picart C, Discher DE. Surface probe measurements of the elasticity of sectioned tissue, thin gels and polyelectrolyte multilayer films: correlations between substrate stiffness and cell adhesion. Surf Sci. 2004; 570(1–2):142–154.
13. Jacot JG, Dianis S, Schnall J, Wong JY. A simple microindentation technique for mapping the microscale compliance of soft hydrated materials and tissues. J Biomed Mater Res A. 2006; 79A(3):485–494. [PubMed: 16779854]
14. Lundkvist, A.; Lilleodden, E.; Siekhaus, W.; Kinney, J.; Pruitt, L.; Balooch, M. Viscoelastic properties of healthy human artery measured in saline solution by AFM-based indentation technique. In: Gerberich, WW.; Gao, H.; Sundgren, JE.; Baker, SP., editors. Thin films: stresses and mechanical properties, VI. Pittsburg: MRS; 1997. p. 353-357.
15. Oie T, Murayama Y, Fukuda T, Nagai C, Omata S, Kanda K, et al. Local elasticity imaging of vascular tissues using a tactile mapping system. J Artif Organs. 2009; 12(1):40–46. [PubMed: 19330504]
16. Ebenstein DM, Pruitz LA. Nonoindentation of biological materials. Nanotoday. 2006; 1(3):26–33.
17. Peloquin J, Huynh J, Williams RM, Reinhart-King CA. Indentation measurements of the subendothelial matrix in bovine carotid arteries. J Biomech. 2011; 44(5):815–821. [PubMed: 21288524]

18. Engler AJ, Griffin MA, Sen S, Bonnemann CG, Sweeney HL, Discher DE. Myotubes differentiate optimally on substrates with tissue-like stiffness: pathological implications for soft or stiff microenvironments. J Cell Biol. 2004; 166(6):877–887. [PubMed: 15364962]
19. Matsumoto T, Abe H, Ohashi T, Kato Y, Sato M. Local elastic modulus of atherosclerotic lesions of rabbit thoracic aortas measured by pipette aspiration method. Physiol Meas. 2002; 23(4):635. [PubMed: 12450265]
20. Zhang A-J, Yu X-J, Wang M. The clinical manifestations and pathophysiology of cerebral small vessel disease. Neurosci Bull. 2010; 26(3):257–264. [PubMed: 20502505]
21. Klein R, Knudtson M, Klein B, Zinman B, Gardiner R, Suissa S, et al. The relationship of retinal vessel diameter to changes in diabetic nephropathy structural variables in patients with type 1 diabetes. Diabetologia. 2010; 53(8):1638–1646. [PubMed: 20437026]
22. Gama Sosa MA, Gasperi RD, Rocher AB, Wang AC-J, Janssen WGM, Flores T, et al. Age-related vascular pathology in transgenic mice expressing presenilin 1-associated familial alzheimer's disease mutations. Am J Pathol. 2010; 176(1):353–368. [PubMed: 20008141]
23. Sorokin L. The impact of the extracellular matrix on inflammation. Nat Rev Immunol. 2010; 10(10):712–723. [PubMed: 20865019]
24. Karuri NW, Liliensiek S, Teixeira AI, Abrams G, Campbell S, Nealey PF, et al. Biological length scale topography enhances cell-substratum adhesion of human corneal epithelial cells. J Cell Sci. 2004; 117(15):3153–3164. [PubMed: 15226393]
25. Liliensiek SJ, Campbell S, Nealey PF, Murphy CJ. The scale of substratum topographic features modulates proliferation of corneal epithelial cells and corneal fibroblasts. J Biomed Mater Res A. 2006; 79(1):185–192. [PubMed: 16817223]
26. Ingram DA, Mead LE, Tanaka H, Meade V, Fenoglio A, Mortell K, et al. Identification of a novel hierarchy of endothelial progenitor cells using human peripheral and umbilical cord blood. Blood. 2004; 104(9):2752–2760. [PubMed: 15226175]
27. Barakat A, Lieu D. Differential responsiveness of vascular endothelial cells to different types of fluid mechanical shear stress. Cell Biochem Biophys. 2003; 38(3):323–343. [PubMed: 12794271]
28. Radmacher M, Tillamnn R, Fritz M, Gaub H. From molecules to cells: imaging soft samples with the atomic force microscope. Science. 1992; 257(5078):1900–1905. [PubMed: 1411505]
29. Pelham RJ, Wang Y-L. Cell locomotion and focal adhesions are regulated by substrate flexibility. PNAS. 1997; 94(25):13661–13665. [PubMed: 9391082]
30. Radmacher M, Fritz M, Kacher CM, Cleveland JP, Hansma PK. Measuring the viscoelastic properties of human platelets with the atomic force microscope. Biophys J. 1996; 70(1):556–567. [PubMed: 8770233]
31. Love A. Bussinesq's problems for a rigid cone. Q J Math. 1939; 10:161–175.
32. Radmacher, M. Studying the mechanics of cellular processes by atomic force microscopy. In: YuLi, W.; Dennis, ED., editors. Methods in cell biology. AP: 2007. p. 347-372.
33. McKee CT, Wood JA, Shah NM, Fischer ME, Reilly CM, Murphy CJ, et al. The effect of biophysical attributes of the ocular trabecular meshwork associated with glaucoma on the cell response to therapeutic agents. Biomaterials. 2011; 32(9):2417–2423. [PubMed: 21220171]
34. Soofi SS, Last JA, Liliensiek SJ, Nealey PF, Murphy CJ. The elastic modulus of matrigel$^{(TM)}$ as determined by atomic force microscopy. J Struct Biol. 2009; 167(3):216–219. [PubMed: 19481153]
35. Last JA, Liliensiek SJ, Nealey PF, Murphy CJ. Determining the mechanical properties of human corneal basement membranes with atomic force microscopy. J Struct Biol. 2009; 167(1):19–24. [PubMed: 19341800]
36. Akhtar R, Schwarzer N, Sherratt MJ, Watson REB, Graham HK, Trafford AW, et al. Nanoindentation of histological specimens: mapping the elastic properties of soft tissues. J Mater Res. 2009; 24(3):638–646. [PubMed: 20396607]
37. Thompson MT, Berg MC, Tobias IS, Rubner MF, Van Vliet KJ. Tuning compliance of nanoscale polyelectrolyte multilayers to modulate cell adhesion. Biomaterials. 2005; 26(34):6836–6845. [PubMed: 15972236]
38. Meyers J, Craig J, Odde David J. Potential for control of signaling pathways via cell size and shape. Curr Biol. 2006; 16(17):1685–1693. [PubMed: 16950104]

39. Ingber DE. Fibronectin controls capillary endothelial cell growth by modulating cell shape. PNAS. 1990; 87(9):3579–3583. [PubMed: 2333303]

40. Form DM, Pratt BM, Madri JA. Endothelial cell proliferation during angiogenesis. Lab Invest. 1986; 55(5):521–530. [PubMed: 2430138]

41. Madri JA, Pratt BM, Yannariello-Brown J. Matrix-driven cell size changes modulates aortic endothelial cell proliferation and sheet migration. Am J Pathol. 1988; 132(1):18–27. [PubMed: 3394798]

42. Barakat AI. Responsiveness of vascular endothelium to shear stress: potential role of ion channels and cellular cytoskeleton (review). Int J Mol Med. 1999; 4(4):323–332. [PubMed: 10493972]

43. Nakashima Y, Raines EW, Plump AS, Breslow JL, Ross R. Upregulation of VCAM-1 and ICAM-1 at atherosclerosis-prone sites on the endothelium in the apoE-Deficient Mouse. Arterioscler Thromb Vas Biol. 1998; 18(5):842–851.

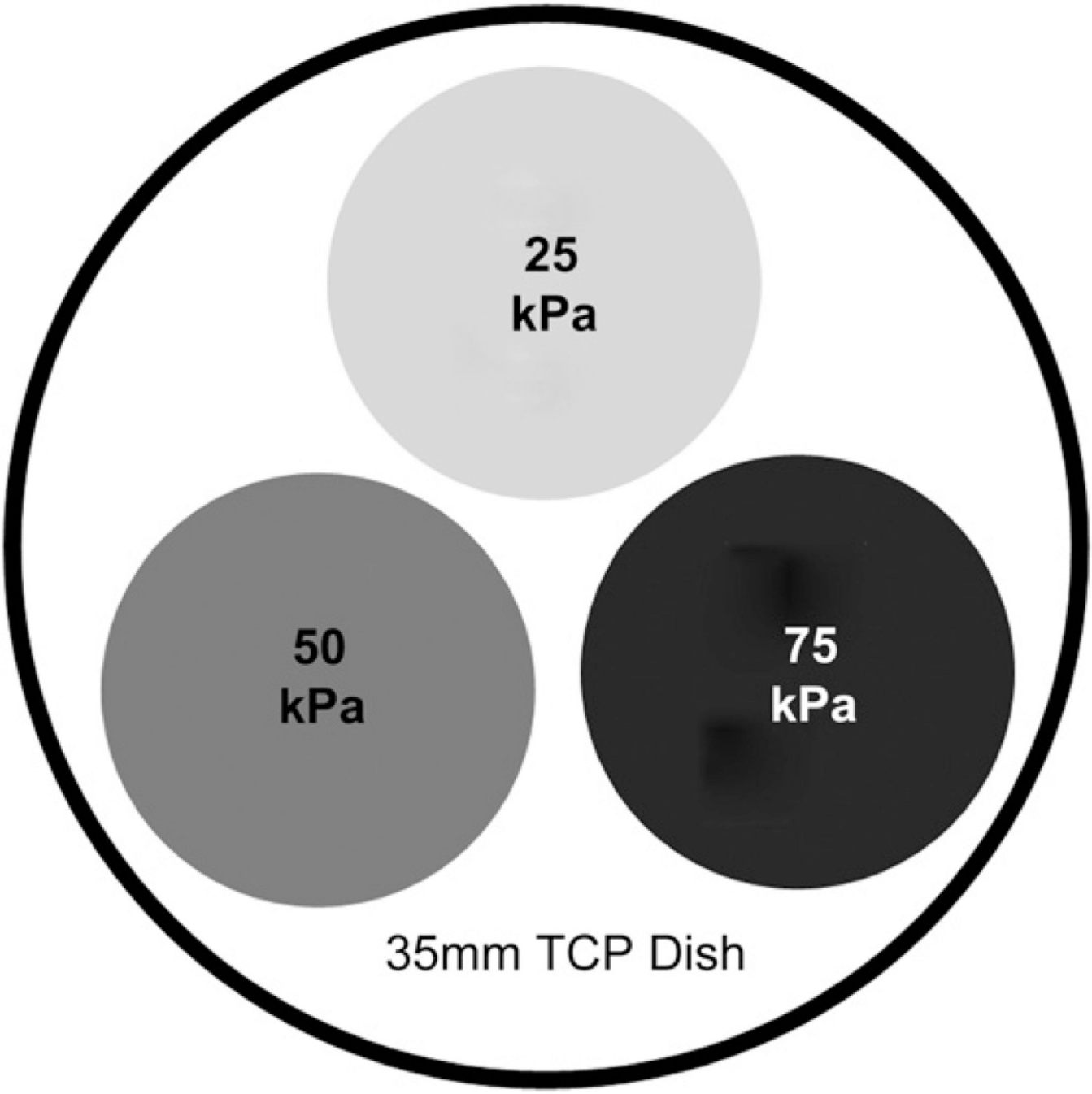

Fig. 1.
Triple-pack gel dish. Gel substrates of each compliance value (25, 50 and 75 kPa) were cut using a ⅜; inch punch and adhered inside a 35 mm TCP dish. Gels were allowed to adhere to the surface of the dish for 5 min, followed by hydration with 5 mL of 1x PBS.

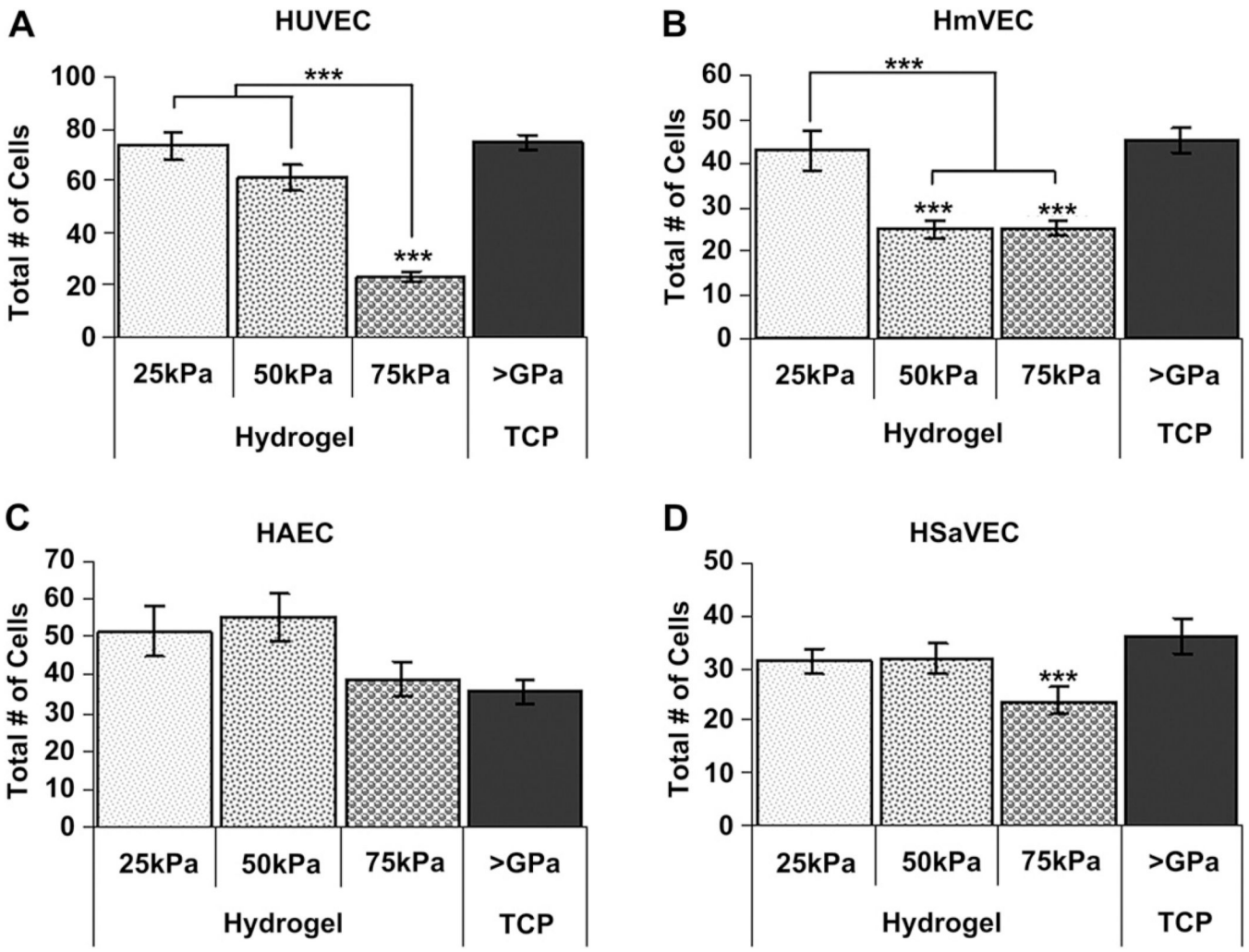

Fig. 2.

Cell attachment 24 h after seeding as a function of substrate compliance. Significantly fewer HUVECs (A) attached to the 75 kPa surfaces compared to the 25 kPa, 50 kPa, and TCP surfaces. Similarly, fewer HmVECs (B) attached to the 75 kPa and 50 kPa surfaces compared to the 25 kPa surfaces. Attachment of HmVECs to the TCP surfaces was comparable to the 25 kPa surfaces. For the arterial endothelial cell population, HAEC (C), no significant differences were found in cell density. Interestingly, the TCP surfaces also had a lower cell density compared to the softer compliance surfaces. The saphenous vein endothelial cells, HSaVEC (D) had significantly fewer cells on the 75 kPa surfaces compared to the TCP surfaces and fewer cells than the 25 kPa or 50 kPa surfaces. All data are presented as mean ± SEM. ***(* = $p < 0.05$, ** = $p < 0.01$, *** = $p < 0.001$).

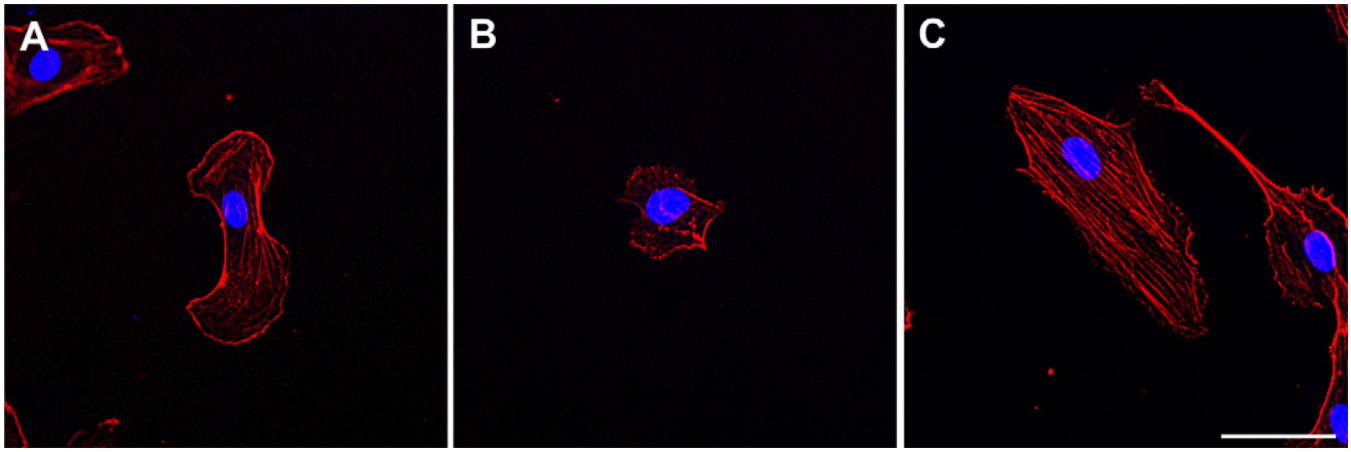

Fig. 3.

Substratum modulus influences endothelial cell area, elongation and cytoskeletal dynamics. Representative images of HUVECs seeded on 75 kPa substrates (B) are both smaller and more rounded than cells on either 25 kPa substrates (A) or TCP (C). Actin (phalloidin stain, red) labeling demonstrates fewer stress fibers on softer 25 kPa and 75 kPa substrates as compared to TCP (>1 GPa). Nuclear (DAPI) labeling is seen in blue. Scale bar = 50 μm.

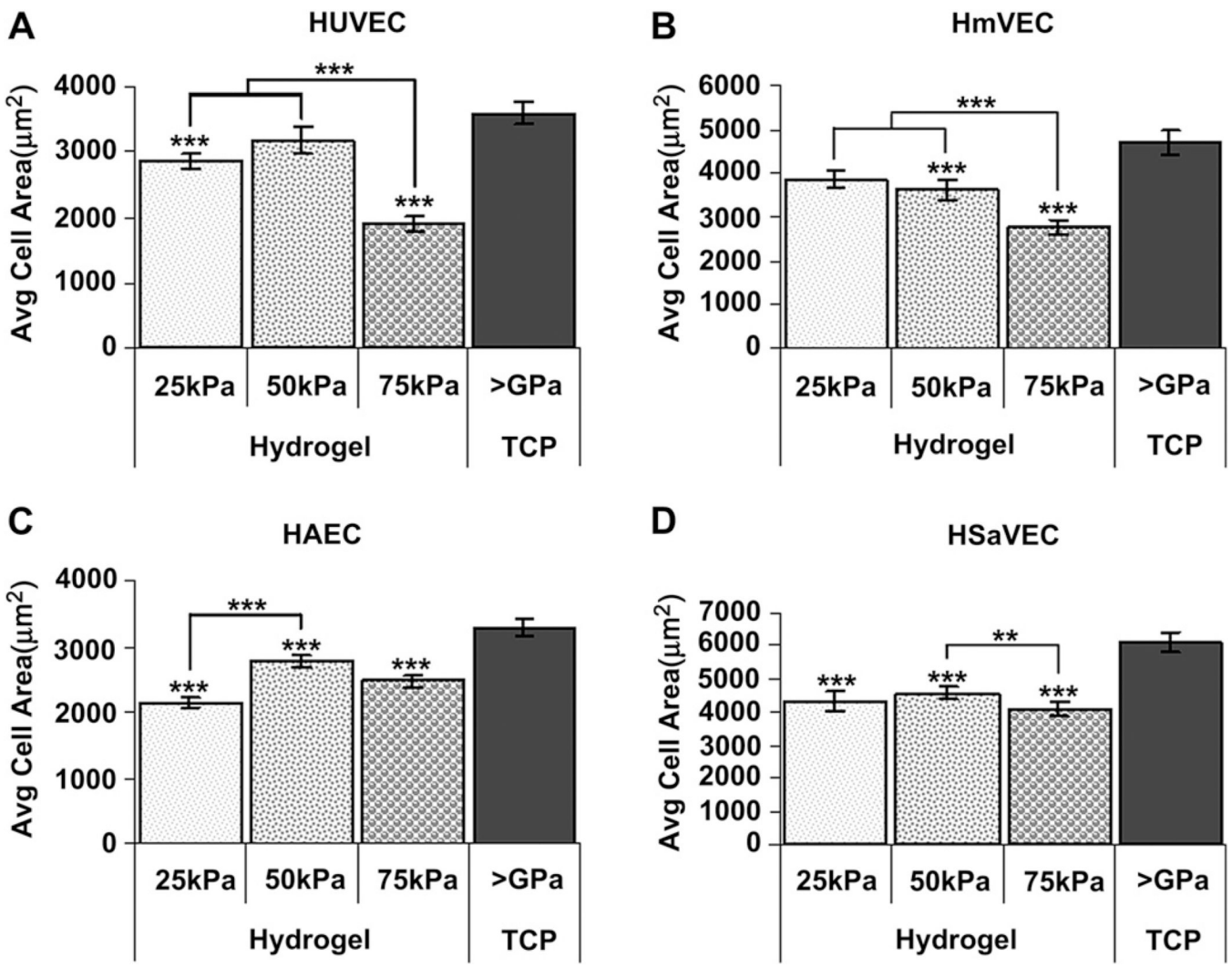

Fig. 4.

Cell area 24 h after seeding as a function of substrate compliance. HUVECs (A) seeded onto 75 kPa surfaces were significantly smaller than those cells seeded onto 25 kPa, 50 kPa, and TCP surfaces. HUVECs seeded onto 25 kPa surfaces were also significantly smaller than cells seeded onto TCP surfaces. HmVECs (B) demonstrated a similar pattern as the HUVECs with significantly smaller cells on the 75 kPa surfaces as compared to the 25 kPa, 50 kPa, and TCP. HmVECs seeded onto 50 kPa surfaces were also significantly smaller than cells seeded onto TCP surfaces. HAECs (C) seeded onto 25 kPa, 50 kPa, and 75 kPa surfaces were significantly smaller than cells seeded on to TCP surfaces. HAECs seeded onto 25 kPa surfaces were also significantly smaller then those seeded on to 50 kPa surfaces. HSaVECs (D) seeded onto 25 kPa, 50 kPa, and 75 kPa surfaces were significantly smaller than those cells seeded onto TCP surfaces. HSaVECs seeded onto 75 kPa surfaces are also significantly smaller than cells seeded on to 50 kPa surfaces. All data are presented as the mean ± SEM. (* = $p < 0.05$, ** = $p < 0.01$, *** = $p < 0.001$).

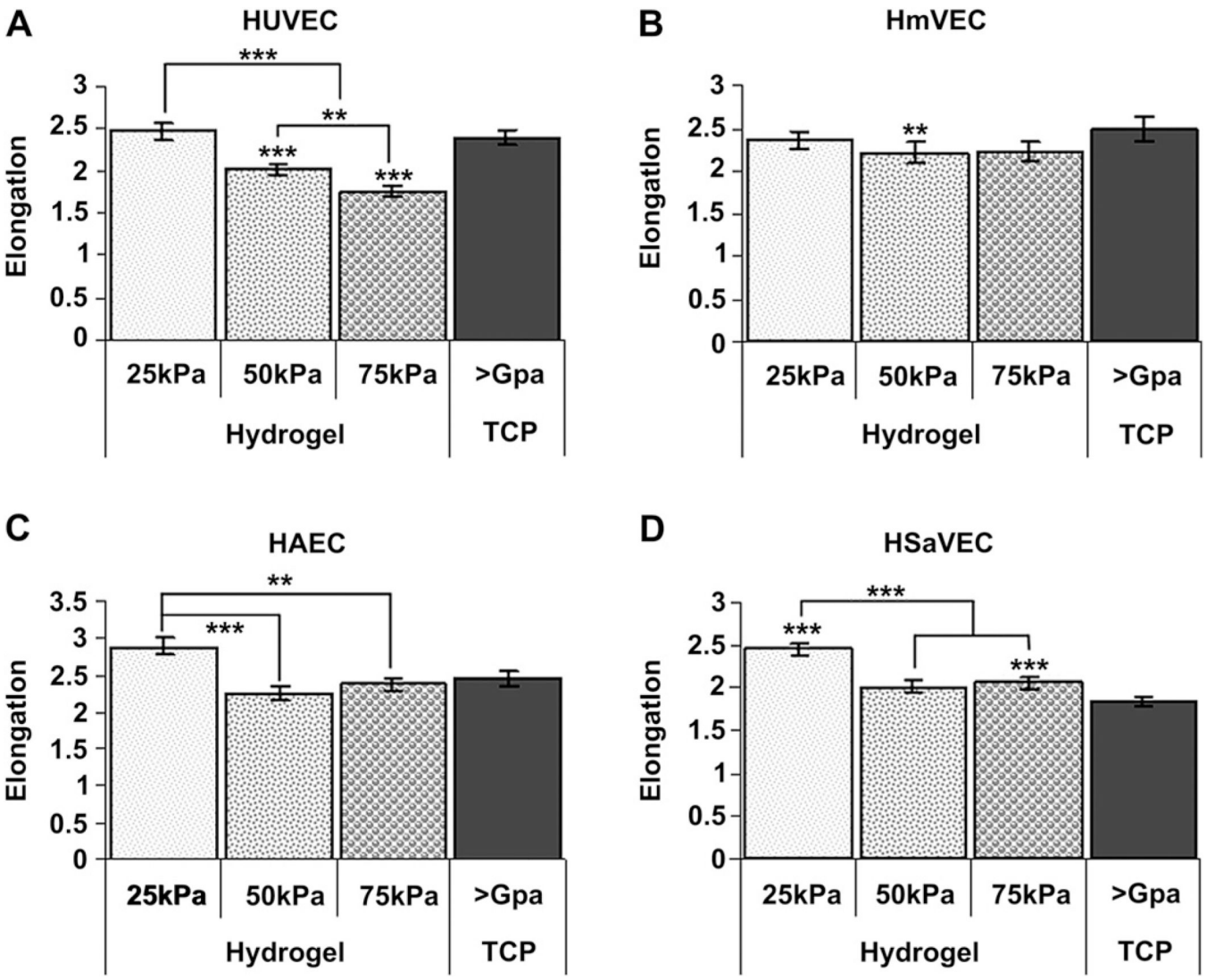

Fig. 5.

Cell elongation 24 h after seeding as a function of substrate compliance. HUVECs (A) seeded onto 75 kPa and 50 kPa surfaces were significantly more rounded than those cells seeded onto 25 kPa, and TCP surfaces. HUVECs seeded onto 75 kPa surfaces were also significantly more rounded than cells seeded onto 50 kPa surfaces. HmVECs (B) seeded onto 50 kPa surfaces were significantly more rounded than cells seeded on to TCP surfaces but not 75 kPa or 25 kPa surfaces. HAECs (C) seeded onto 25 kPa surfaces were significantly more elongated than cells seeded onto 50 kPa and 75 kPa surfaces. For HAECs on 25 kPa surfaces there was trend to be more elongated than those on TCP surfaces but the differences did not reach statistical significance. HSaVECs (D) seeded onto 25 kPa surfaces were significantly more elongated than cells on 50 kPa, 75 kPa, and TCP surfaces. HSaVECs seeded onto 75 kPa surfaces were also significantly more elongated than cells seeded onto TCP surfaces. Cells on 50 kPa surfaces tended to be more elongated than those on TCP surfaces but did not reach statistical significance. All data are presented as the mean ± SEM. (* = $p < 0.05$, ** = $p < 0.01$, *** = $p < 0.001$).

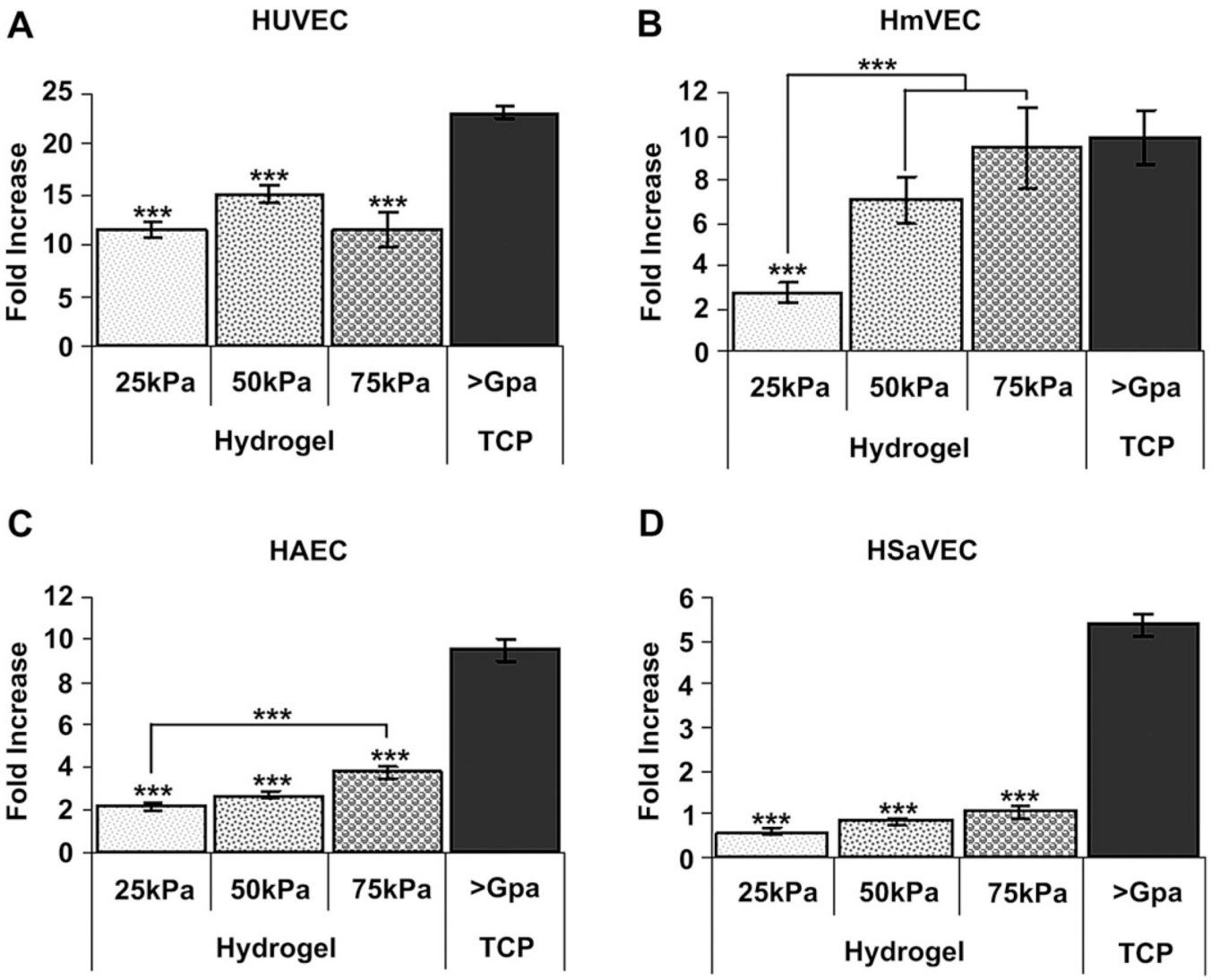

Fig. 6.

Cell proliferation as a function of substrate compliance. HUVECs (A) seeded onto TCP surfaces grew much more rapidly than those cells seeded onto 25 kPa, 50 kPa, and 75 kPa surfaces. HmVECs (B) seeded onto 25 kPa surfaces grew significantly more slowly than cells seeded onto 50 kPa, 75 kPa, and TCP surfaces. Similar to HUVECs, HAECs (C) seeded on to TCP surfaces grew significantly more rapidly than cells seeded onto 25 kPa, 50 kPa, and 75 kPa surfaces. Additionally, HAECs seeded onto 75 kPa surfaces grew significantly more rapidly than cells seeded onto 25 kPa surfaces. HSaVECs (D) seeded onto TCP surfaces grew significantly more rapidly than cells on 25 kPa, 50 kPa, and 75 kPa surfaces. All data are presented as fold increase of the mean ± SEM. (* = $p < 0.05$, ** = $p < 0.01$, *** = $p < 0.001$).

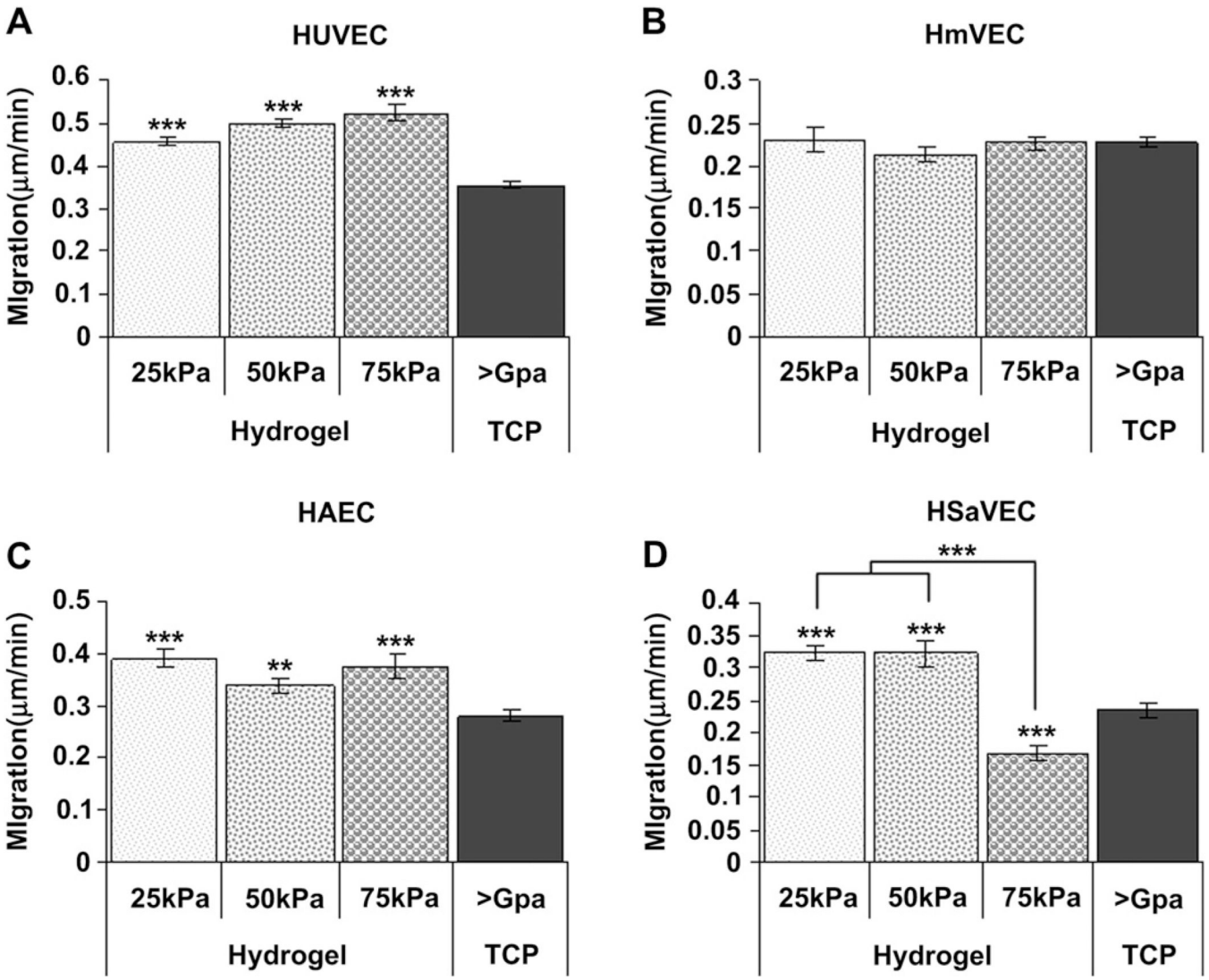

Fig. 7.

Cell migration as a function of substrate compliance. HUVECs (A) seeded onto TCP surfaces migrated at a significantly slower rate than those cells seeded onto 25 kPa, 50 kPa, and 75 kPa surfaces. HmVECs (B) migration rates did not vary significantly between the 25 kPa, 50 kPa, 75 kPa or TCP surfaces. HAECs (C) seeded onto TCP surfaces migrated at a significantly slower rate than cells seeded onto 25 kPa, 50 kPa, and 75 kPa surfaces. HSaVECs (D) seeded onto 25 kPa and 50 kPa surfaces migrated at a significantly higher rate than cells on 75 kPa and TCP surfaces. Additionally, HSaVECs on 75 kPa surfaces migrated at a significantly slower rate than cells on TCP surfaces. All data are presented as the mean ± SEM. (* = $p < 0.05$, ** = $p < 0.01$, *** = $p < 0.001$).